

# Verification of the optical system performance of FIFI-LS: the field-imaging far-infrared line spectrometer for SOFIA

Mario Schweitzer<sup>a</sup>, Albrecht Poglitsch<sup>a</sup>, Walfried Raab<sup>a</sup>, Randolph Klein<sup>b</sup>, Rainer Hönle<sup>a</sup>, Norbert Geis<sup>a</sup>, Reinhard Genzel<sup>a</sup>, Leslie W. Looney<sup>c</sup>, M. Hamidouche<sup>c</sup>, Thomas K. Henning<sup>d</sup>

<sup>a</sup>Max-Planck-Institut für extraterrestrische Physik, Garching, Germany

<sup>b</sup>University of California, Berkeley, USA

<sup>c</sup>University of Illinois, Urbana-Champaign, USA

<sup>d</sup>Max-Planck-Institut für Astronomie, Heidelberg, Germany

## ABSTRACT

FIFI-LS is a Field-Imaging Line Spectrometer designed for the SOFIA airborne observatory. The instrument will operate in the far infrared (FIR) wavelength range from 42 to 210  $\mu\text{m}$ . Two spectrometers operating between 42-110  $\mu\text{m}$  and 110-210  $\mu\text{m}$  allow simultaneous and independent diffraction limited 3D imaging over a field of view of 6'' x 6'' and 12'' x 12'' respectively. We have developed a telescope simulator to test the imaging and spectral performance of FIFI-LS in the FIR. Here, we present the telescope simulator as well as the performance verification of FIFI-LS using the simulator. Finally we compare the measurements with the theoretical expected performance of FIFI-LS.

**Keywords:** Integral Field Spectroscopy, Spectrometer, Airborne Astronomy, FIFI, FIFI-LS, SOFIA

## 1. INTRODUCTION

The FIR Field Imaging Line Spectrometer (FIFI-LS<sup>1-4</sup>) is one of the nine first generation instruments. It is selected for the first scientific flight campaigns of the airborne observatory SOFIA. It is an integral field spectrometer which allows to simultaneously obtain both a two dimensional image of an astronomical object and spectral information for each spatial pixel. The instrument covers a wavelength range from 42 to 210  $\mu\text{m}$ .

The spectral information of different regions within the image of an astronomical object is a powerful tool to investigate the physical conditions in the astronomical source. The wavelength range of FIFI-LS covers many important spectral features, e.g. atomic fine structure lines ([OI] 63 & 145  $\mu\text{m}$ , [OIII] 53 & 88  $\mu\text{m}$ , [NII] 122 & 205  $\mu\text{m}$ , [NIII] 57  $\mu\text{m}$ , [CII] 158  $\mu\text{m}$ ) or emission lines from molecules such as OH, H<sub>2</sub>O, CH, and CO and many other molecular species. This spectral information can be used to investigate e.g. the morphology of heating and cooling in nearby galaxies, the powering mechanism and ISM chemistry of ultra luminous infrared galaxies (ULIRGs) or to investigate active galactic nuclei (AGN) where CO cooling lines, arising from a hot torus, are expected.

### 1.1 Optics Design

Although a detailed discussion of the optical design of FIFI-LS can be found in another volume of the Proceedings of SPIE,<sup>5</sup> we will briefly review the overall optical system here. As mentioned above, FIFI-LS is a two channel spectrometer that allows simultaneous observations in the wavelength bands 42 - 110  $\mu\text{m}$  and 110 - 210  $\mu\text{m}$ . The two spectrometer channels share a common entrance optics which is used for image de-rotation as well as re-focusing of the light onto the slicer mirrors. The entrance optics and a chopped dual-temperature calibration source are mounted in the liquid nitrogen area of the instrument. The two, otherwise independent, spectrometers are separated right after entering the liquid helium area at the Lyot-stop by exchangeable multi layer interference dichroics. The only difference in both spectrometer bands is a set of re-imaging mirrors that doubles the image size on the blue image slicer resulting in a close to diffraction limited pixel size of 12'' in the long wavelength and 6'' in the short wavelength spectrometer.

An image slicer system in each wavelength band rearranges the two dimensional 5x5 pixel field of view along a one dimensional pseudo slit, forming the entrance slit to the grating spectrometer. Littrow mounted diffraction

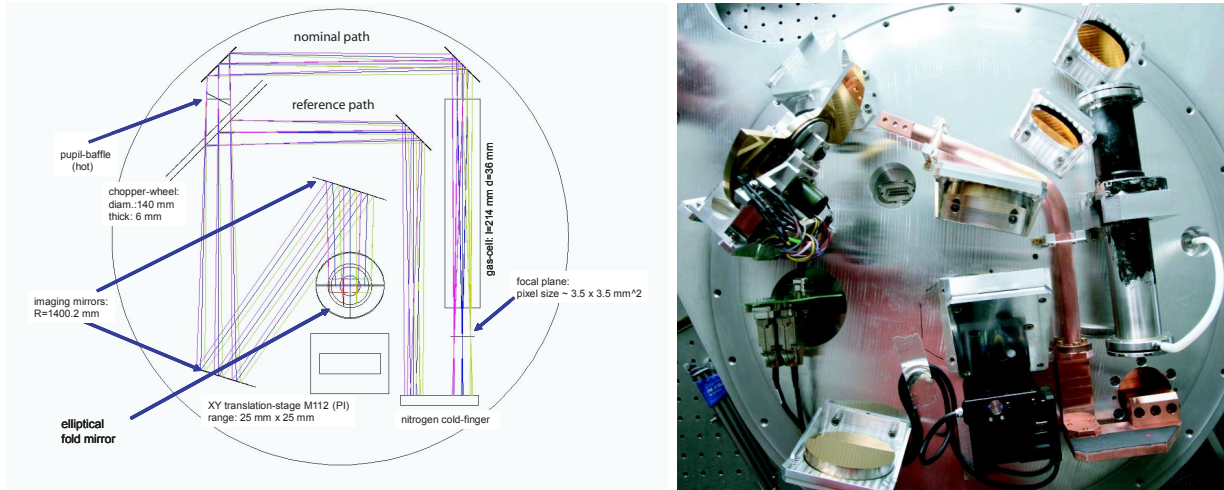


Figure 1. Left: ray tracing simulation of the telescope simulator. Right: photo of the telescope simulator.

gratings optimized for the respective waveband are used for spectral multiplexing in each spectrometer band. The grating in the red spectrometer, covering one octave in wavelength, is operated in first diffraction order only. The blue grating has to be operated in first and second order to fully cover the blue wavelength band. The calculated efficiency of the red grating peaks at  $148 \mu\text{m}$  reaching an efficiency of  $\sim 98\%$ , while the blue grating, optimized for two diffraction orders, only reaches a peak efficiency of around  $75\%$  at  $55 \mu\text{m}$  (1st order) and  $90 \mu\text{m}$  (2nd order), respectively.

After returning from the Littrow spectrometers, the spectra are re-imaged onto the detector arrays by anamorphic exit optics with the appropriate magnification in the spectral and spatial dimension. Light cones attached in front of the individual pixel provide area filling coverage of the focal plane.

To verify the instrument performance of FIFI-LS (spatial resolution, spectral resolution and spectral calibration) in the FIR a telescope simulator was build. The telescope simulator reproduces the SOFIA FIR telescope beam. This is necessary in order to test whether the optical path of FIFI-LS is well aligned with respect to the optical axis of the SOFIA telescope using the SOFIA mounting flange/plane as a reference. The optical performance of all FIFI-LS components can be tested at their working temperatures and in the FIR. Furthermore, the telescope simulator allows us to characterize the spectral and imaging properties of FIFI-LS.

## 2. THE TELESCOPE SIMULATOR

In order to test the spectral performance, the telescope simulator has a gas cell mounted into the optical path that can be filled from outside the telescope simulator (e.g. with CO at room temperature). The gas cell provides FIR molecular emission lines, since it is mounted in front of a cold background. It can be used to spectrally calibrate the instrument and to measure the spectral resolution of FIFI-LS. To test the imaging properties of FIFI-LS, a FIR point source is scanned through the field of view. This allows one to test the optics. By scanning the point source across the field of view, a beam map can be obtained that delivers the point spread function (PSF) of the instrument. In addition, a cooled infrared black mask can be brought into the pupil to homogeneously illuminate the entire detector array.

Figure 1 presents the ray tracing simulation of the telescope simulator and a photo of the actual telescope simulator. An XY-translation stage that is integrated in the telescope simulator, allows one to move a point source (Fig. 2) in two dimensions across the focal plane. The point source is a gold plated spherical segment with a diameter of 2 mm, which is fixed with two thin suspension wires. The detector pixel size in the focal plane of the telescope simulator is about  $3.5 \times 3.5 \text{ mm}^2$ . The suspension wires ( $30 \mu\text{m}$  in diameter) are fixed to a holding clamp mounted on the XY-translation stage. Behind the focal plane, a copper plate is located in the optical path. This plate is connected via a copper rod to a vessel which is filled from outside of the telescope

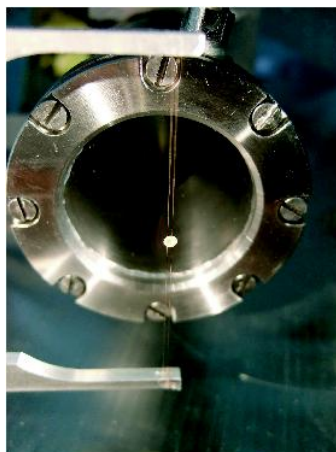


Figure 2. A gold plated spherical segment of 2 mm in diameter serves as a point source by reflecting the ambient room temperature radiation into the optical path of FIFI-LS. A liquid nitrogen cooled background plate produces the necessary contrast.

simulator with liquid nitrogen. The rest of the telescope simulator is at room temperature. The gold plated spherical segment in the focal plane reflects the ambient room temperature radiation into the optical path of FIFI-LS. The copper plate is painted black with an infrared black paint. This cool background produces the contrast necessary to see the warm reflected room temperature radiation as a FIR point source. Using the telescope simulator an automated point source scan can be performed to measure the PSF of FIFI-LS within the entire field of view. The size of the scan region, the number of positions within this region, and the waiting time at each single position have to be entered into the control program of the telescope simulator before the scan is started. To be able to identify the single detector readouts with the proper motor positions, the FIFI-LS computers and the computer controlling the telescope simulator are synchronized by their CPU times. FIFI-LS marks each read-out with a time stamp, and the telescope simulator marks each point source position with a start and an end time that is written into an additional file. In this way, the data can be correlated with the individual point source positions.

To achieve a meaningful observation in the FIR it is necessary to subtract the ambient background radiation from the actual observation. At the SOFIA telescope, the secondary mirror is used to chop the field of view on and off the source. This is necessary since the background radiation in the FIR (e.g. due to the warm telescope and to the remaining atmosphere emission) is in general high. The telescope simulator offers the possibility to obtain chopped observations using a chopper, shown in Figure 1. The chopper mirror rotates, thus switching between two optical paths. The nominal optical path is seen if the chopper mirror is out of the beam. In this configuration FIFI-LS has a direct view onto the focal plane and the point source with the cooled copper plate in the background. When the chopper mirror is inside the beam, the reference path is selected. The reference path uses two additional flat mirrors to achieve a direct view onto the cooled copper plate, excluding the point source. Using the reference path, a background image can be acquired which can be subtracted from the actual observation. This solves the problem of a dominant and potentially time varying background.

It is important that the rotation of the chopper mirror is synchronized with the readout sequence of FIFI-LS. After the synchronization the data collection can start. The data are stored in a sequence of nominal path and reference path observations, with the readout sequence of FIFI-LS controlled by the so called "pattern generator". The pattern generator also provides a TTL (Transistor-Transistor-Logic) signal that can be used for the synchronization. Figure 1 shows the chopper wheel and the light switches, which are mounted in front of the chopper wheel. Two light switches mounted under  $45^\circ$  with respect to each other detect the rotation frequency of the chopper wheel and its phase. Frequency and phase are then compared to the frequency and phase of the pattern signal using a PLL (phased locked loop) circuit which controls the synchronization. After a short time ( $\sim 10$  seconds) a stable, synchronized rotation is achieved. The simulator uses two light switches simultaneously

to increase the sampling rate, so that for low rotation frequencies the PLL circuit is still able to synchronize the rotation with the pattern signal.

Using the gas cell (Fig.1), FIFI-LS can be spectrally calibrated and characterized. The gas cell can be brought into the beam of the nominal optical path. Its windows are made from a thin polypropylene foil. The length of the gas cell is 214 mm and its diameter is 36 mm. A tube connects the cell to the outer part of the telescope simulator. The tube is used to bring a gas (e.g. CO or ambient air) into the gas cell. For a line measurement, the point source is moved out of the field of view. Since we have a warm (room temperature), optically thin gas ( $\sim 20$  mbar) in front of a cool background ( $\sim 70$  K), the gas shows molecular emission features.

Before any measurement with the telescope simulator is performed, the optical axis of the telescope simulator has to be well aligned with respect to the optical axis of FIFI-LS. A warm (room temperature) pupil mask is located at the pupil position of the telescope simulator, which can be used to align the two axes with respect to each other. The mask has a centered hole with exactly the size of the pupil. If the two axes were misaligned, the outer warm rim of the pupil mask would enter the beam of FIFI-LS, increasing drastically the FIR background signal of all detectors. By aligning a fold mirror located between the telescope simulator and FIFI-LS, the FIR background signal can be minimized. In this way, the two optical axes can be aligned with respect to each other.

### 3. PERFORMANCE VERIFICATION OF FIFI-LS

The spectral and imaging properties of FIFI-LS were tested in two cool downs, during which we performed measurements with the telescope simulator. We performed a point source scan across the field of view to measure the PSF of FIFI-LS. In order to measure the spectral resolution and to achieve a spectral calibration, the gas cell was filled under low pressure ( $\sim 20$  mbar) with air of ambient humidity (or carbon monoxide) while at the same time a grating scan was performed. The results of these measurements are presented in the following sections.

#### 3.1 The Spatial Resolution

First, FIFI-LS and the telescope simulator were evacuated and cooled to their working temperatures. Prior to any measurement the rotation of the chopper mirror has to be phase locked to the pattern signal (readout sequence). This synchronization was found to be stable after an initial settling time of about 10 seconds. The phase between chopper position and FIFI-LS readout was set by optimizing the time delay between the pattern signal and the actual FIFI-LS readout. For the measurements we have chosen 4 ramps (time integrated signals) per half cycle of the chopper mirror. The first readout was taken along the nominal beam. The second/fourth readout was recorded while the chopper mirror moved in/out of the beam so that the signal became weaker/stronger with time. These ramps were not used in the data processing. The third readout was taken along the reference beam (no source), so that the total signal was weaker than for the nominal beam. The third ramp (reference beam) was subtracted from the first ramp (nominal beam) to achieve a subtraction of the background signal.

In Figure 3, the background-subtracted  $5 \times 5$  pixel field of view of FIFI-LS is shown, with the point source located on the central pixel. Multiple ramps were co-added to produce this image. The source seems to be elongated along the horizontal direction. This effect is due to the thermal radiation/reflection of the suspension wires of the source and was also observed in the point source scan (als shown in Fig. 3).

The grating was in its center position corresponding to a wavelength of  $\sim 160 \mu\text{m}$ . The full width at half maximum of the PSF of FIFI-LS is expected to be not significantly larger than the pixel size. This is due to compromises made in the optical design with respect to diffraction effects. To measure the PSF with a reasonable spatial sampling rate, it is necessary to scan the point source with small spatial steps across the field of view while recording the spectrally collapsed signal for each spatial pixel simultaneously. The step width of the point source was  $\sim 1.35$  mm (corresponding to 0.39 pixel) and the integration time (waiting time) at each position was 5 seconds. The single point source positions are indicated in Figure 3 by the black dots. As was previously observed (Fig. 3 (left)), an elongated structure is detected (in y-direction). This structure can be explained by the infrared signal produced by the suspension wires of the source. To take this underlying signal into account the measurement was fitted using the superposition of a two-dimensional and second one-dimensional Gaussian

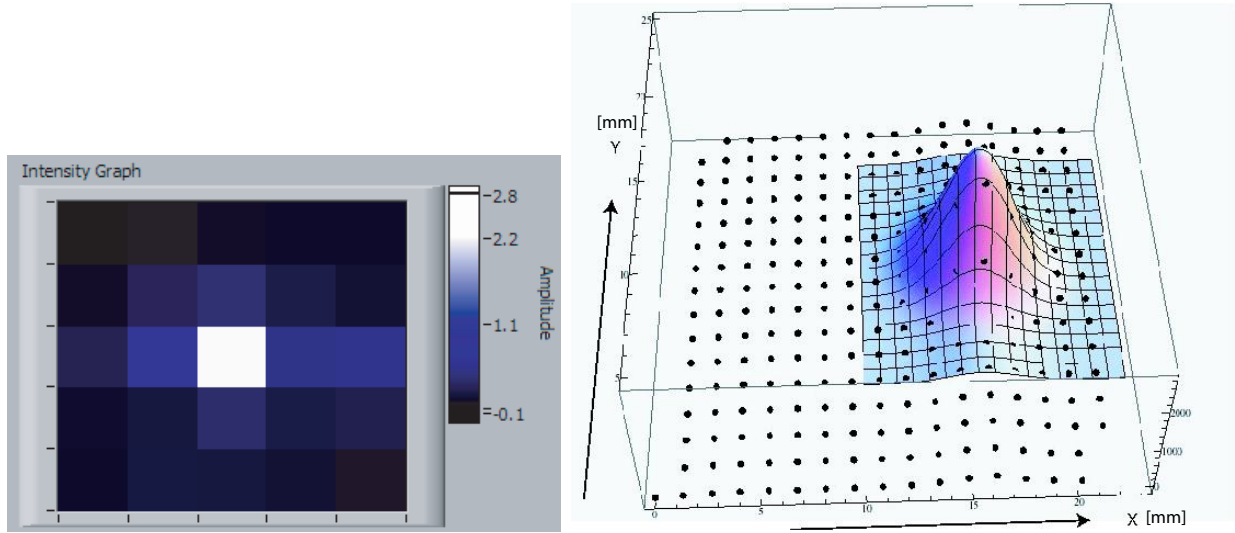


Figure 3. Left:  $5 \times 5$  pixel field of view of FIFI-LS with centered point source. Right: spectrally collapsed signal of one spatial pixel versus the position of the point source.

$$model = a \cdot e^{-0.5\left[\left(\frac{x-x_0}{\sigma_x}\right)^2 + \left(\frac{y-y_0}{\sigma_y}\right)^2\right]} + b \cdot e^{-0.5\left(\frac{x-x_0}{\sigma_x}\right)^2} + c. \quad (1)$$

The fit result is shown in Figure 3. The resulting fit parameters are :  $a = 2663.2$  ,  $b = 258.3$  ,  $c = -42.8$  ,  $x_0 = 15.9$  ,  $y_0 = 16.5$  ,  $\sigma_x = 1.7$  ,  $\sigma_y = 1.5$  with  $x_0, y_0, \sigma_x, \sigma_y$  given in mm, while  $a, b, c$  are given in arbitrary units. For the full width at half maximum in the x direction, we obtained  $FWHM_x \sim 4.1$  mm and in y direction  $FWHM_y \sim 3.6$  mm. Due to a magnification factor of  $\sim 1.037$  between the detector plane of FIFI-LS and the focal plane of the telescope simulator this result translates into  $FWHM_x \sim 4.3$  mm and  $FWHM_y \sim 3.7$  mm in the detector plane of FIFI-LS. The magnification factor has been determined using a ray tracing simulation and verified by measuring the intensity distribution (as in Fig. 3) for separate pixels. A difference in the FWHM between the x and y directions is expected and caused by the fact that the slicer mirrors of the image slicer unit cut more light out of the diffraction pattern along their short side (y-direction) than along their extended side. The lower transmission for the energy within the wings of the point source diffraction pattern in the y-direction tends to decrease the FWHM of the PSF in this direction.

For FIFI-LS, a detailed scalar diffraction analysis was performed with the software package GLAD.<sup>6</sup> A simulated diffraction pattern for a monochromatic point source was calculated in the detector plane of FIFI-LS. The FWHM along the spatial direction was 4.3 mm, measured from a cut through the diffraction pattern as shown in Figure 4. Since the pixel size (3.6 mm) of the detector is similar to the FWHM of the PSF, the intensity distribution of the diffraction pattern has to be convolved with the pixel size of the detector. This slightly increases the FWHM. Taking also the difference for the transmission in the horizontal and vertical direction of the slicer mirrors into account, the expected FWHM in the detector plane is  $FWHM_x \sim 4.9$  mm and  $FWHM_y \sim 4.5$  mm. The difference of the FWHM of the PSF between the two directions is  $\sim 8\%$  of the larger FWHM. A comparison to the measured FWHM of the PSF shows that the measured FWHM is slightly smaller, while the difference between the two directions is  $\sim 14\%$  of the larger FWHM.

While the agreement between the simulation and the measurement is generally good, the small deviations may be explained by the error within the magnification factor, a somewhat different diffraction situation within the simulator compared to the SOFIA telescope, and a slightly smaller effective pixel size caused by the behavior of the light-cones located in front of each pixel. Also, a slightly different wavelength, due to a small deviation from the center position of the grating, may contribute to the deviation between measurement and calculation.

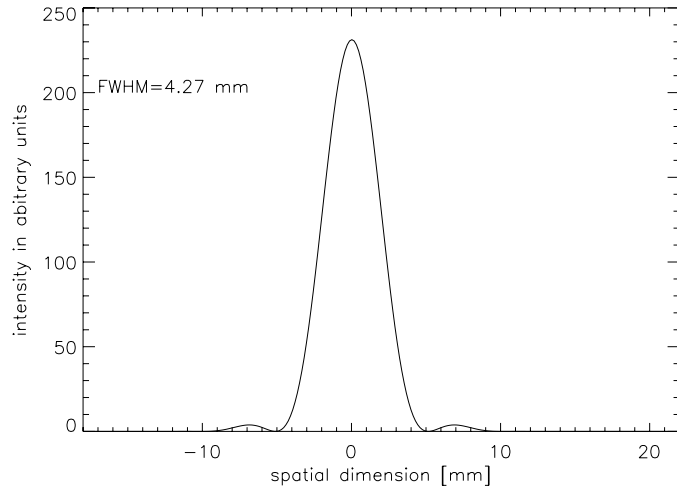


Figure 4. Cut (spatial direction) through the simulated diffraction pattern of a monochromatic point source in the detector plane of FIFI-LS.

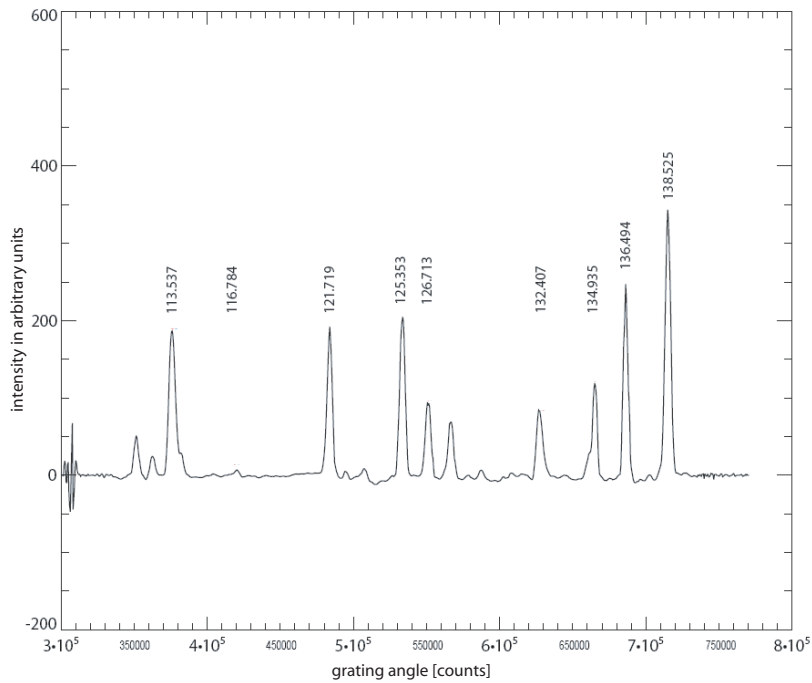


Figure 5. Measured water spectrum with the x-axis given in counts of the grating position readout. The y-axis is given in arbitrary units. The numbers above the lines indicate the wavelength values taken from the literature in micrometers.

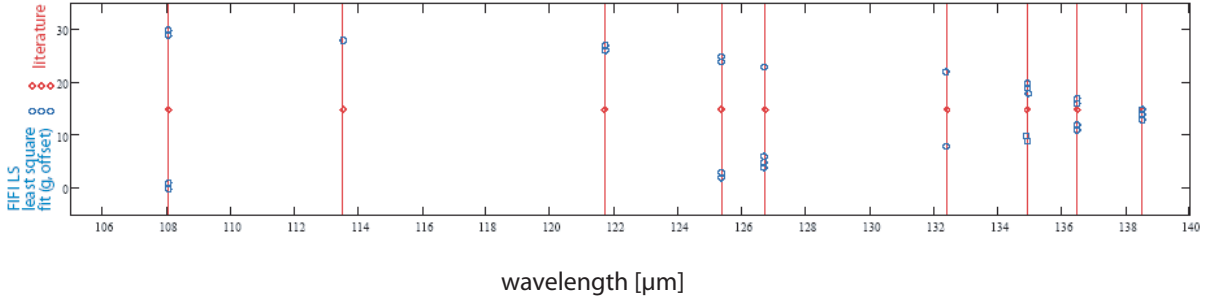


Figure 6. Spectral calibration using the water lines from Figure 5. The red lines indicate the wavelength values for the lines taken from the literature. The blue circles indicate the fitted wavelength values, taking the grating position readouts and a consistent set of fit parameters into account. The vertical axis indicates the chronological order of the individual line measurements within the grating scan.

### 3.2 The Spectral Calibration

To perform the spectral calibration, the point source was moved out of the field of view and the gas cell was mounted into the nominal beam. The gas cell was connected to a vacuum pump with an additional valve to fill air or carbon monoxide into the cell. Both gases have strong transition lines in the wavelength range of FIFI-LS. The gas cell was filled with laboratory air under a pressure of  $\sim 20$  mbar. The 16 spectral pixels of the central detector module (center of the field of view) were used to perform a first order spectral calibration of the instrument. Individual water lines (due to rotational transitions) were identified by comparing the pattern of the measured versus expected water lines and used for the spectral calibration of FIFI-LS. The measured spectrum is shown in Figure 5, where several water lines were identified. The x-axis of Figure 5 shows the position readout for the grating angle (in counts). The y-axis shows the flux density in arbitrary units. The numbers above the lines indicate the wavelength values taken from the literature in  $\mu\text{m}$ . To achieve the spectral calibration, we fitted the measured grating positions for the centroid of a line to its theoretical wavelength using the grating equation. This has been performed for all the lines with a single, consistent set of fit parameters. As fit parameters, we assumed a variable grating period  $g'$  in mm/groove to account for the thermal contraction of the grating. Due to the uncalibrated offset of the grating position readout a constant angle offset  $\alpha$  from the actual measured position is also considered. The grating equation holds for the central spectral pixel (center of detector). To determine the wavelength of lines which were not centered on the detector we took a wavelength shift  $\Delta\lambda_{(pixel-dispersion)}$  into account, the so called pixel dispersion. Thus the grating equation for the Littrow-setup can be written as

$$\lambda(g', m, \phi + \alpha, \gamma) = \frac{g'}{m}(\sin(\phi + \alpha + \gamma) + \sin(\phi + \alpha - \gamma)) + \Delta\lambda_{(pixel-dispersion)}, \quad (2)$$

where  $m$  is the diffraction order,  $\phi$  the Littrow angle,  $\gamma=0.75^\circ$  the deviation from the perfect Littrow configuration. The pixel dispersion  $\Delta\lambda_{(pixel-dispersion)}$  was calculated using the following relation

$$\Delta\lambda_{(pixel-dispersion)}(g', m, \phi, \gamma) = \frac{d}{d\phi} \left( \frac{g'}{m}(\sin(\phi + \gamma) + \sin(\phi - \gamma)) \right) \cdot \text{pixscal} \cdot \Delta_{pixel}. \quad (3)$$

Here  $\text{pixscal}$  is a conversion factor converting the incident angle  $\phi$  into pixels at the detector. This value has been determined using a ray tracing simulation.  $\Delta_{pixel}$  is the centroid shift of the line in pixels with respect to the center of the detector. The fit result is shown in Figure 6. The red lines indicate the wavelength values for the lines taken from the literature. The blue circles indicate the fitted wavelength values, determined using the grating position readouts and a consistent set of fit parameters. One set of fit parameters ( $g' = 0.117$  mm,  $\alpha = 20.957^\circ$ ) was sufficient to fit all lines very well with a standard deviation of  $\sigma = 0.014\mu\text{m}$ .

### 3.3 The Spectral Resolution

To determine the spectral resolution of FIFI-LS, we measured the CO line at  $162.81 \mu\text{m}$  ( $J=16-15$ ) at a gas pressure of about 20 mbar and at room temperature by scanning the grating (Fig. 7). For this measurement

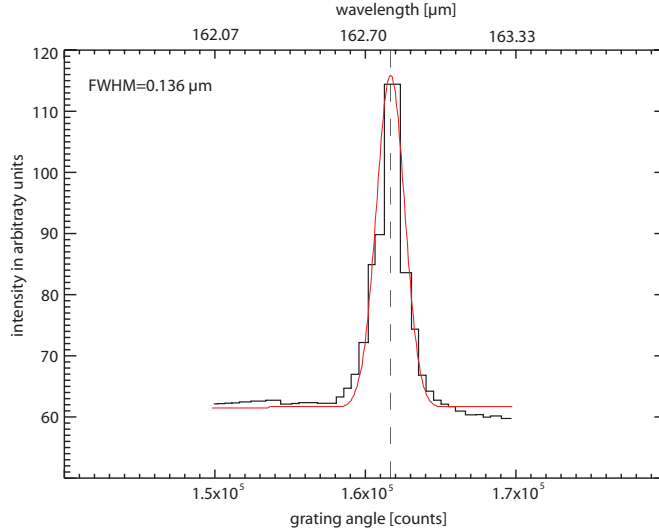


Figure 7. CO line (J=16-15 at 162.81  $\mu\text{m}$ ) measurement + Gaussian fit with the x-axis given in counts of the grating position readout (with arbitrary offset). The y-axis is given in arbitrary units.

Property	Expectation	Measurement
FWHM of the PSF (at detector)	$4.9 \times 4.5 \text{ mm}$	$4.3 \times 3.7 \text{ mm}$
spectral resolution (at 160 $\mu\text{m}$ )	R=1268	R=1200
spectral calibration		achieved ( $g' = 0.117 \text{ mm}$ , $\alpha = 20.957^\circ$ )

Table 1. Comparison of expected and measured instrument properties.

we used CO gas at low pressure to prevent the blending of emission lines and minimize the pressure broadening. While the grating was performing the scan, the signal of the central detector pixel was recorded. A Gaussian function was fitted to the measured line, and the FWHM of the line was found to be  $\sim 0.136 \mu\text{m}$ . It follows that the spectral resolution is  $R = \frac{\Delta\lambda}{\lambda} \sim 1200$ . The theoretically expected value can be calculated using the following equation for the approximation of a Littrow-configuration, where the incident and the exit beam coincide

$$R_{theo} = m \cdot N = \frac{m \cdot g \cdot \text{coll}}{\cos(\beta)} = \frac{m \cdot g \cdot \text{coll}}{\sqrt{1 - (m \cdot g \cdot 0.5\lambda)^2}}. \quad (4)$$

Here  $m$  is the diffraction order,  $N$  describes the number of illuminated grating grooves,  $g$  describes the groove density in grooves/mm (grating constant),  $\text{coll}$  is the diameter of the collimated beam,  $\beta$  the angle of incidence and  $\lambda$  the wavelength (in our setup,  $m=1$ ,  $g=8.5$  grooves/mm,  $\text{coll}=120 \text{ mm}$  and  $\lambda \sim 163 \mu\text{m}$ ). The expected resolution is then  $R_{theo} = 1414$ . This value is just slightly larger than the measured resolution. The difference can be understood if we take into account that we did not consider the discrete pixel sampling in Equation 4. To correct for this effect, the continuous intensity distribution has to be convolved with the pixel size in the focal plane ( $3.6 \times 3.6 \text{ mm}^2$ ). The discrete pixel sampling slightly increases the  $\Delta\lambda$  by a factor of 1.115 (see also<sup>7</sup>) at 160  $\mu\text{m}$ , so  $R_{theo-discrete} = 1268$ . This is in good agreement with the measured resolution. Finally, Table 1 summarizes the results and compares the expected and measured properties.

#### 4. CONCLUSIONS

We introduced the function of a telescope simulator which we have designed to test the spectral and imaging properties of FIFI-LS in the FIR. Performing measurements with the telescope simulator we found a good agreement between the expected and measured properties of FIFI-LS. Using the telescope simulator we measured the spatial resolution of FIFI-LS by scanning a FIR point source through the field of view. In addition a gas-cell

(filled with air or CO) has been used to measure the spectral resolution and calibrate the wavelength scale of FIFI-LS.

- For the FWHM of the PSF we found  $\text{FWHM}_x \sim 4.3$  mm and  $\text{FWHM}_y \sim 3.7$  mm in the detector plane of FIFI-LS while the calculated values are  $\text{FWHM}_x \sim 4.9$  mm and  $\text{FWHM}_y \sim 4.5$  mm. The small deviations may be explained by the error within the magnification factor (between the focal plane of FIFI-LS and telescope simulator), a somewhat different diffraction situation within the simulator compared to the SOFIA telescope, and a slightly smaller effective pixel size caused by the behavior of the light-cones located in front of each pixel. Also a slightly different wavelength, due to a small deviation from the center position of the grating, may contribute to the deviation between measurement and calculation.
- Using the gas-cell (filled with laboratory air), we achieved a spectral calibration of FIFI-LS. Multiple water lines were identified from the measured line pattern and used for the calibration. To perform the calibration, we fitted the measured grating positions for the centroids of the lines to their theoretical wavelengths using the grating equation and a consistent set of fit parameters. As fit parameters, we assumed a variable grating period  $g'$  in mm/groove to account for the thermal contraction of the grating. Due to the uncalibrated offset of the grating position readout a constant angle offset  $\alpha$  from the actual measured position is also considered. The final calibration was successfully achieved with  $g' = 0.117$  mm and  $\alpha = 20.957^\circ$ .
- To determine the spectral resolution of FIFI-LS the CO line at  $163 \mu\text{m}$  (J=16-15) at a gas pressure of about 20 mbar was measured at room temperature. The FWHM of the CO line has been measured to  $\sim 0.136 \mu\text{m}$ . This corresponds to a resolution of  $R = 1200$  which agrees quite well with the calculated resolution of  $R = 1268$ .

## REFERENCES

- [1] Geis, N., Poglitsch, A., Raab, W., Rosenthal, D., Kettenring, G., and Beeman, J. W., "FIFI LS: a field-imaging far-infrared line spectrometer for SOFIA," in [*Proc. SPIE Vol. 3354, p. 973-984, Infrared Astronomical Instrumentation, Albert M. Fowler; Ed.*], Fowler, A. M., ed., *Presented at the Society of Photo-Optical Instrumentation Engineers (SPIE) Conference 3354*, 973–984 (Aug. 1998).
- [2] Looney, L. W., Geis, N., Genzel, R., Park, W. K., Poglitsch, A., Raab, W., Rosenthal, D., Urban, A., and Henning, T., "Realizing 3D spectral imaging in the far-infrared: FIFI LS," in [*Proc. SPIE Vol. 4014, p. 14-22, Airborne Telescope Systems, Ramsey K. Melugin; Hans-Peter Roeser; Eds.*], Melugin, R. K. and Roeser, H.-P., eds., *Presented at the Society of Photo-Optical Instrumentation Engineers (SPIE) Conference 4014*, 14–22 (June 2000).
- [3] Rosenthal, D., Beeman, J. W., Geis, N., Looney, L. W., Poglitsch, A., Park, W. K., Raab, W., and Urban, A., "16 x 25 Ge:Ga detector arrays for FIFI LS," in [*Proc. SPIE Vol. 4014, p. 156-163, Airborne Telescope Systems, Ramsey K. Melugin; Hans-Peter Roeser; Eds.*], Melugin, R. K. and Roeser, H.-P., eds., *Presented at the Society of Photo-Optical Instrumentation Engineers (SPIE) Conference 4014*, 156–163 (June 2000).
- [4] Klein, R., Poglitsch, A., Raab, W., Geis, N., Hamidouche, M., Looney, L. W., Hönle, R., Schweitzer, M., Viehhauser, W., Genzel, R., Haller, E. E., and Henning, T., "FIFI LS: the far-infrared integral field spectrometer for SOFIA," in [*Ground-based and Airborne Instrumentation for Astronomy. Edited by McLean, Ian S.; Iye, Masanori. Proceedings of the SPIE, Volume 6269, pp. 62691F (2006).*], *Presented at the Society of Photo-Optical Instrumentation Engineers (SPIE) Conference 6269* (July 2006).
- [5] Raab, W., Poglitsch, A., Looney, L. W., Klein, R., Geis, N., Hoenle, R., Viehhauser, W., Genzel, R., Hamidouche, M., Henning, T., and Haller, E. E., "FIFI LS: the far-infrared integral field spectrometer for SOFIA," in [*Ground-based Instrumentation for Astronomy. Edited by Alan F. M. Moorwood and Iye Masanori. Proceedings of the SPIE, Volume 5492, pp. 1074-1085 (2004).*], Moorwood, A. F. M. and Iye, M., eds., *Presented at the Society of Photo-Optical Instrumentation Engineers (SPIE) Conference 5492*, 1074–1085 (Sept. 2004).
- [6] Raab, W., Poglitsch, A., Klein, R., Hoenle, R., Schweizer, M., Viehhauser, W., Geis, N., Genzel, R., Looney, L. W., Hamidouche, M., Henning, T., and Haller, E. E., "Characterizing the system performance of FIFI LS: the field-imaging far-infrared line spectrometer for SOFIA," in [*Ground-based and Airborne Instrumentation*

for Astronomy. Edited by McLean, Ian S.; Iye, Masanori. *Proceedings of the SPIE, Volume 6269*, pp. 62691G (2006).], Presented at the Society of Photo-Optical Instrumentation Engineers (SPIE) Conference **6269** (July 2006).

- [7] Raab, W., Looney, L. W., Poglitsch, A., Geis, N., Hoenle, R., Rosenthal, D., and Genzel, R., “FIFI LS: the optical design and diffraction analysis,” in [*Airborne Telescope Systems II. Edited by Ramsey K. Melugin, Hans-Peter Roeser . Proceedings of the SPIE, Volume 4857*, pp. 166-174 (2003).], Melugin, R. K. and Roeser, H.-P., eds., Presented at the Society of Photo-Optical Instrumentation Engineers (SPIE) Conference **4857**, 166–174 (Feb. 2003).